

# Rigorous Versus Generalized Sensor Models: Assessment of Different Height Sources for Orthorectification of High-Resolution Satellite Imagery

**Ali A. El Sagheer, Khaled M. Zaki,  
Mahmoud S. Gomaa, and Ayman M. Marrei**

**ABSTRACT:** The main aim of this research is to investigate the impact of vertical accuracy of digital elevation models (DEMs) on the orthoimage production process. The study took place on a QuickBird image by using four different DEMs with different vertical accuracies, nine ground control points (GCPs), and three sensor models. The four DEMs are global positioning system (GPS)-based DEM, topographic map-based DEM, Shuttle Radar Topography Mission-based DEM, and advanced spaceborne thermal emission and reflection-based DEM. The used sensor models are the rigorous sensor model, rational functional model (RFM), and refined RFM. The results show that the RFM without GCPs gives inaccurate results especially in case of high spatial resolution satellite images. The research recommends using the rigorous model and the refined RFM for orthorectifying images accurately as the results showed that these two models give accurate, precise, and stable results. As well, their results do not contain systematic errors.

**KEYWORDS:** Sensor models, high-resolution satellite imagery, orthoimage, DEM, QuickBird, GCPs, SRTM, ASTER, RFM and rigorous model

## Introduction

To obtain orthorectification to very high-resolution imagery, whatever the raw data format, it is necessary to follow the following steps: (1) acquisition of images and metadata; (2) acquisition of the coordinates X, Y, and Z of ground control points (GCPs) and independent check points (IChkPs); (3) obtaining the image coordinates of these points; (4) computation of the unknown parameters of the 3D geometric correction model used; and (5) images orthorectification process using a digital elevation model (DEM) (Aguilar et al. 2005). The role of DEM is to eliminate terrain-induced displacement so as to transform a central perspective to an orthogonal projection (Li et al. 2002),

as the orthorectification process transforms the central projection of the image into an orthogonal view of the ground with a uniform scale, thereby removing the distortion caused by terrain relief (Junfeng and Jinfeng 2006). DEM quality is a very important element of the orthorectification process as it can greatly influence the accuracy of planimetry in orthoimages (Junfeng and Jinfeng 2006). Sensor models are a key component to represent the functional relationships between the image space and the object space, and are essential for single/multi-imagery orientation (Li et al. 2009). Sensor models can be grouped into two classes, physical (rigorous or parametric) sensor models and generalized (generic or nonparametric) sensor models (Tao et al. 2000). The choice of a sensor model depends primarily on the performance and accuracy required, and the sensor and control information available (Tao and Hu 2001). Generalized sensor models are generic, that is, their parameters do not carry physical meanings of the imaging process. Generally, it is not essential to know sensor's geometry for using generic models and it is possible to use them for different types of sensors (Hosseini 2008).

---

**Ali A. EL Sagheer, Khaled M. Zaki, Mahmoud S. Gomaa, and Ayman M. Marrei**, Shoubra Faculty of Engineering, Surveying Department, Benha University, Banha, Egypt. Tel: 002 0552353186, 002 01118051307, 002 01001336662, and 002 01027609390. E-mails: <ambehairy@gmail.com>, <drkhaledzaky@yahoo.com>, <dr.farag.7@hotmail.com>, and <eng\_msadek2013@yahoo.com>.

---

In a generalized sensor model, the transformation between image and object space is represented as some general function without modeling the physical imaging process. The function can be of several different forms, such as polynomials or rational functions (Hosseini 2008).

## Previous Studies

However, there are few publications that address viability, accuracy, and stability of such models. Tao et al. (2000) test the aerial optical images (frame sensor type). The test results show that both rational function model and polynomial model can reach reasonably good accuracy. Because the fitting accuracy of the cases with four-degree rational functional model (RFM) is almost the same as those with six-degree RFM, high-order forms are often not necessary. The iterative solution method to RFM provides a better accuracy than the direct solution method, but the direct solution method is usually adequate when enough control points are available.

Elashmawy et al. (2005) present two mathematical models for stereo IKONOS imagery restitution. The mathematical models that were used in this research are based on the RFM and the 3D affine projection mode. It was found that sub-meter horizontal accuracy and 1.3-1.7 m vertical accuracy can be obtained using either the refined RFM model or the 3D affine projection model for the stereo images.

Chang et al. (2010) proposed a collocation-aided block adjustment for multisensor images. The direct georeferencing, which is one of the rigorous sensor model (RSM), and the rational function model are combined a mathematical model for block adjustment. Then the least squares collocation is included to compensate the systematic errors for those heterogeneous models. A digital elevation model is used in the block adjustment. The test data set includes GeoEye, QuickBird, WorldView-1, Kompsat-2, and Formosat-2 satellite images. Experimental results indicate that the proposed block adjustment significantly improved both the absolute accuracy and relative discrepancy.

The motivation behind this study is that there are several issues requiring consideration in respect of the orthorectification of satellite imagery: which model performs the best for orthorectification of satellite imagery, how does each model perform with DEMs that have different sources and different accuracies, and

Point	H (m)	h (m)	N (m)	N <sub>mean</sub>
P1	63.739	79.061	15.322	15.3325
P2	57.407	72.750	15.343	

**Table 1.** Determination of the geoidal undulation (N) of the test area.

which DEM incorporated in the orthorectification process contribute to the quality of the results. The objective of this article is to answer these questions, based on an intensive investigation of three models using four DEMs with different accuracies.

## Study Area and Data Sources

The study area has been selected at El-Sayed Nafesa area in Cairo. This area covers approximately  $0.9 \times 0.7$  km and located in the Nile valley zone (the main middle zone) of the plane coordinate system in Egypt. It is an urban area and the terrain varies from 32 to 49 m above the mean sea level.

### Satellite Image

A pan-sharpened image with 0.6 m spatial resolution over the study area was collected in February 2012 by QuickBird-2 satellite (QB02) and supplied in a tagged-image file format (TIFF) digital format. The image is supplied in a product level LV2A and standard product type. This image is radiometrically adjusted by the producer before publishing to improve the image radiometric quality.

### GCPs and ChkPs

To evaluate the planimetric accuracy of the results, 27 GCPs were selected evenly distributed through the study area and well defined on both the image and ground. GPS observations were carried out using the fast-static measuring technique. All points were obtained in the Universal Transverse Mercator (UTM) system, where the projection information is as follows:

Project type	UTM
Reference ellipsoid	WGS-84
Zone number	36

To transform the ellipsoidal heights (h) to orthometric heights (H), the geoidal undulation

Sensor Model	DEM	GCPs	DEM RMSE <sub>Z</sub> (m)	Orthoimage RMSE <sub>XY</sub> (m)	Ratio (RMSE <sub>XY</sub> /RMSE <sub>Z</sub> )
RFM	KGPS-DEM	This sensor model uses no GCPs	2.129	13.684	6.427431
	Topo-DEM		3.581	13.831	3.862329
	SRTM-GDEM		6.228	12.910	2.072897
	ASTER-GDEM		9.780	13.033	1.332618

**Table 2.** Results of the orthorectification process in the case of RFM (RPCs only).

(N) was obtained based on the two benchmarks shown in Table 1 located at about 1.5 km from the study area. In this regard, a digital level was used to determine the orthometric heights of another two fixed points based on the benchmarks. In addition, the ellipsoidal heights (h) of the two fixed points were determined using GPS. Based on the computed orthometric heights and the measured ellipsoidal ones, two values for the geoidal undulation were obtained as illustrated in Table 2. Eventually, the UTM/WGS-84 coordinates of the 27 points were obtained. In the case of planimetric accuracy assessment, 9 points of the 27 were used as GCPs as in Figure 1A, and 11 points were used as check points (ChkPs) as in Figure 1B. In addition, seven points have been discarded because of their relatively high root-mean-square error (RMSE). On the other hand and in the case of vertical accuracy assessment, the whole set of 27 points were used as CPs.

## Digital Elevation Models

To investigate the impact of DEM accuracy on the orthoimage production process, four different sources DEMs with different accuracies have been prepared and tested. By real-time kinematic (GPS-RTK) measuring mode, 4200 points were collected with a horizontal resolution or a grid size of 0.6 m and applied to generate a DEM (Figure 2A. This DEM will be referred to as kinematic GPS (KGPS)-DEM.

Another DEM was prepared by digitizing spot heights on a topographic map for the study area as shown in Figure 2B. The used topographic map has been produced and prepared from aerial photographs acquired in August 1993 at a scale of 1:20000. The DEM was generated with a 0.6-m horizontal resolution. This DEM will be referred to as Topo-DEM.

Shuttle Radar Topography Mission (SRTM) provides a 3 arc-sec (90-m grid size) global DEM

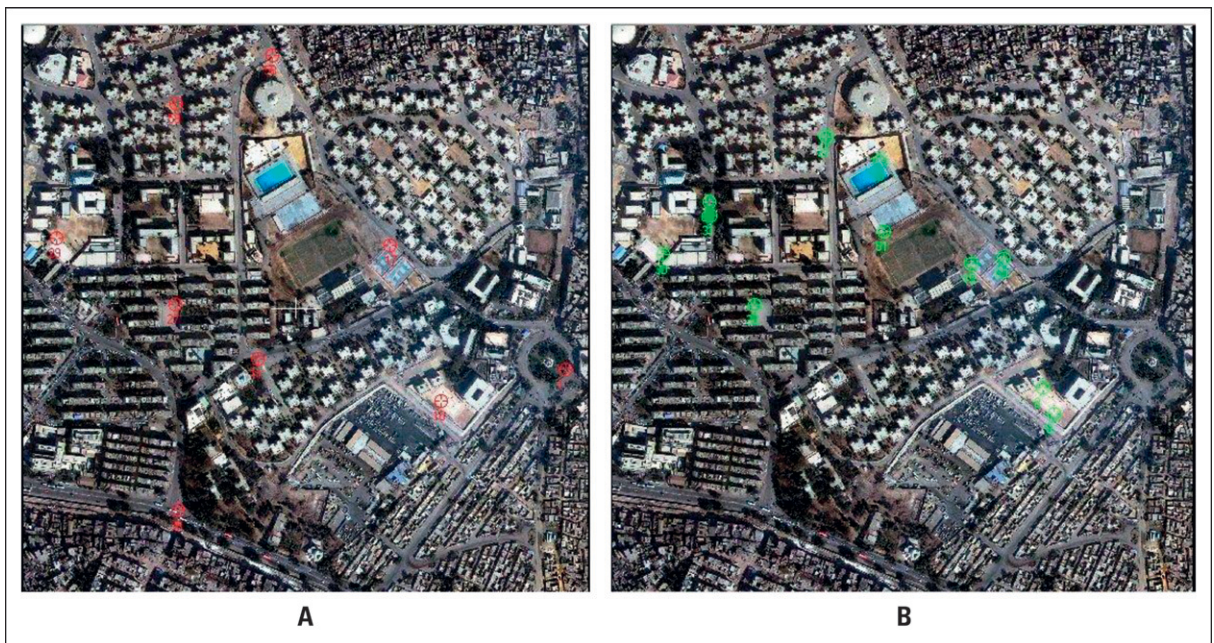


**Figure 1.** Locations of the selected (A) GCPs and (B) ChkPs.

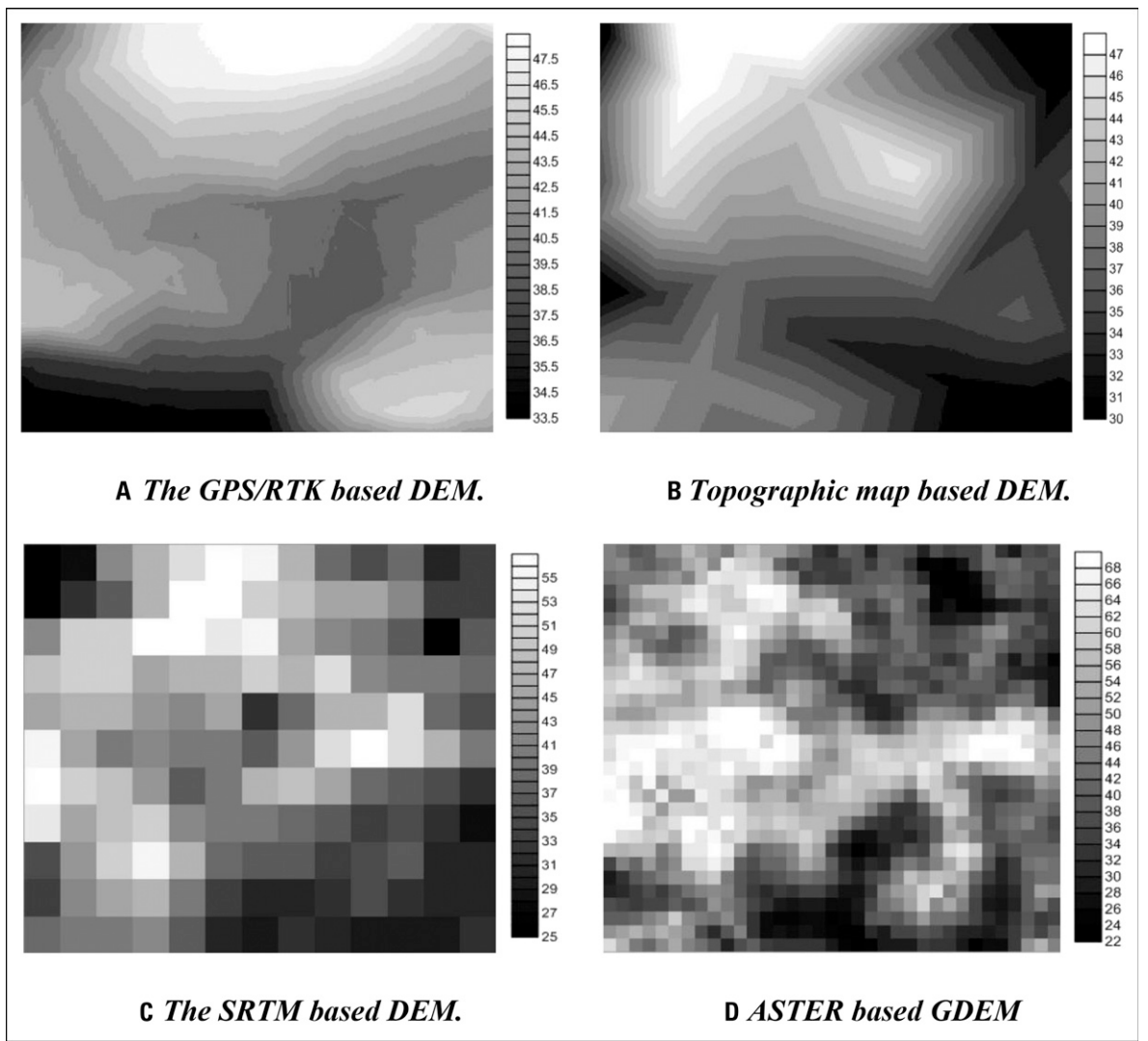


**Figure 2.** The four different sources DEMs.

(GDEM) for free. A one-tile GDEM is obtained. This GDEM is a one-degree angle DEM that covers an area of  $108 \times 108$  km as shown in Figure 2C. After obtaining the SRTM DEM, the data had to be preprocessed using ENVI software to assign the DEM to the UTM/WGS-84 projection system. This DEM will be referred to as SRTM-DEM.

A 30-m advanced spaceborne thermal emission and reflection (ASTER)-GDEM for the study area has been obtained for free. Each ASTER scene covers an area of approximately  $60 \times 60$  km. The data had to be preprocessed using ENVI software to assign the DEM to the UTM/WGS-84 projection system. This DEM shown in Figure 2D will be referred to as ASTER-DEM.

Before starting data processing, the accuracies of the used DEMs were evaluated based on a set of 27 control points. The results show that, the

vertical accuracies, represented by  $RMSE_z$  of the produced DEMs were 2.13, 3.58, 6.23, and 9.78 m for KGPS-DEM, Topo-DEM, SRTM-DEM, and ASTER-DEM, respectively.

## Methodology

In this research, orthorectification of the satellite image has been performed through using three different sensor models: (i) RSM, (ii) RFMs only, and (iii) refined RFMs with GCPs. The input data for the orthorectification process are (i) The QuickBird satellite image of the study area; (ii) nine GCPs evenly distributed through the test area; (iii) four DEMs with different vertical accuracies (KGPS, TOPO, SRTM, and ASTER); and (v) three sensor models (RSM, RFM, and refined

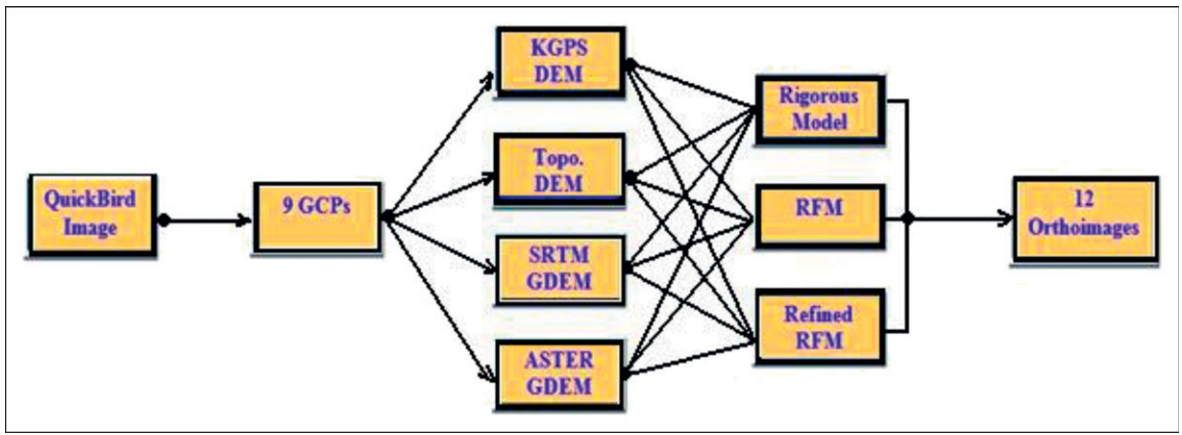


**Figure 3.** The different alternatives for orthorectification process.

RFM). Figure 3 summarizes the different alternatives for the orthorectification process. From Figure 3, it is clearly seen that the experimental work includes 12 alternatives for the orthorectification process.

### Rigorous Sensor Model

A physical sensor model represents the physical imaging process. The parameters involved description of the position and orientation of the sensor with respect to an object space coordinate system. Physical models fully reflect the geometry of viewing (Tao and Hu 2001). Such models are based on platform-specific data, which are the *satellite orbital parameters*, the *attitude angles*, and the *interior orientation parameters* of the sensor. The initial values, possibly provided as metadata, must be refined by estimating their corrections using a suitable number of GCPs (Giannone 2006). This method has a

great robustness over the full image with the use of only a few GCPs (Aguilar et al. 2007). One of the difficulties of rigorous models is their dependency to sensor. As well, for using rigorous models, it is necessary that imaging parameters such as orbital parameters, satellite ephemeris, earth curvature, atmospheric refraction, and lens distortion be known.

### Rational Function Model

RFM based on rational polynomial coefficients (RPCs) is one of the generalized models (Volpe and Rossi 2003). The RFM has better interpolation properties. It is typically smoother and can spread the approximation error more evenly between exact fit points. The RFM has the advantage of permitting efficient approximation of functions that have infinite discontinuities near, but outside, the interval of fitting, while a polynomial approximation is generally unacceptable in this situation. With adequate control information, the RFM can achieve a very high fitting accuracy. This is the primary reason why the RFM has been used as a *replacement sensor model*, Tao and Hu 2001) the major drawbacks of the RFM are the necessity of a large number of GCPs (as they have to guarantee a sufficient redundancy), its high sensitivity to GCPs distribution, and its lack of reliability in the presence of outliers and the possibility of heavy distortions in areas distant from GCPs (Giannone 2006). The RFM expresses each of the  $x$  and  $y$  image coordinates as a ratio of

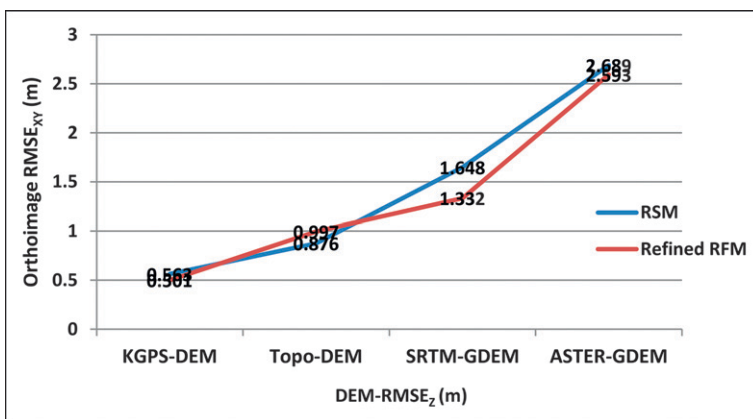


**Figure 4.** The impact of DEM accuracies on the produced orthoimage in the case of rigorous model and refined RFM.

two polynomial functions. It can be represented as follows:

$$x = \frac{P1(X, Y, Z)}{P2(X, Y, Z)} = \frac{\sum_{i=0}^{m1} \sum_{j=0}^{m2} \sum_{k=0}^{m3} a_{ijk} X^i Y^j Z^k}{\sum_{i=0}^{n1} \sum_{j=0}^{n2} \sum_{k=0}^{n3} b_{ijk} X^i Y^j Z^k} \quad (1)$$

$$y = \frac{P1(X, Y, Z)}{P2(X, Y, Z)} = \frac{\sum_{i=0}^{m1} \sum_{j=0}^{m2} \sum_{k=0}^{m3} c_{ijk} X^i Y^j Z^k}{\sum_{i=0}^{n1} \sum_{j=0}^{n2} \sum_{k=0}^{n3} d_{ijk} X^i Y^j Z^k} \quad (2)$$

where  $x$  and  $y$  are image coordinates,  $X$ ,  $Y$ , and  $Z$  ground coordinates,  $a_{ijk}$ ,  $b_{ijk}$ ,  $c_{ijk}$ , and  $d_{ijk}$  polynomial coefficients (total 80), and  $m_1$ ,  $m_2$ ,  $m_3$ ,  $n_1$ ,  $n_2$ ,  $n_3$  ranges from 0 to 3, where  $i + j + k \leq 3$ .

Tao et al. (2000) describes in details how the RFM works.

### RFMs with GCPs

Usually, the RF model is generated based on a RSM. After a rigorous sensor bundle adjustment is performed, multiple evenly distributed image/object grid points can be generated and used as control points (CPs). Then, the rational function coefficients (RFCs) are calculated by these points (Di et al. 2003). A least-squares approach is used to estimate the RFM model coefficients (RPCs) from a 3D pseudo grid of points and orientation parameters. Because sensor orientation is directly observed, there would be some systematic error in orientation parameters. Thus the *refinement* of RFM is required. First, we use the ground coordinate of GCP to compute the

image coordinate through RFM. Second, we determine the affine coefficient by two sets of image coordinates as shown in equation (3). Finally, we refine the result of RFM through affine coefficients (Wu et al. 2008).

$$\text{Sample}_{\text{GCP}} = a_0 + a_1 \cdot \text{Sample}_{\text{RFM}} + a_2 \cdot \text{Line}_{\text{RFM}} \quad (3)$$

$$\text{Line}_{\text{GCP}} = b_0 + b_1 \cdot \text{Sample}_{\text{RFM}} + b_2 \cdot \text{Line}_{\text{RFM}} \quad (4)$$

where  $\text{Sample}_{\text{GCP}}$  and  $\text{Line}_{\text{GCP}}$  are image coordinates of GCP,  $\text{Sample}_{\text{RFM}}$  and  $\text{Line}_{\text{RFM}}$  are image coordinates determined by RFM, and  $a_0$ - $b_2$  are affine coefficients.

## Results and Analysis

To figure out the impact of DEM accuracy on the orthorectification process, the planimetric accuracies of the produced orthoimages were analyzed considering the applied sensor model. In case of the RFM, Table 3 shows that the planimetric accuracies of the produced orthoimages are not accurate, not precise, and not stable. One possible reason is that the RFM depends on ratios of polynomials. The coefficients of the polynomials (RPCs), which are provided with the image, are only approximate values. These results indicate that without GCPs, RFM cannot be used to orthorectify images when accurate results are expected.

A significant improvement was recorded in case of the RSM. The  $\text{RMSE}_{XY}$  ranges from 0.03 to 1.23 m while the absolute shift in north direction

Sensor Model	DEM	GCPs	DEM $\text{RMSE}_Z$ (m)	Orthoimage $\text{RMSE}_{XY}$ (m)	Ratio ( $\text{RMSE}_{XY}/\text{RMSE}_Z$ )
RSM	KGPS-DEM	9	2.129	0.563	0.265
	Topo-DEM		3.581	0.876	0.245
	SRTM-GDEM		6.228	1.648	0.265
	ASTER-GDEM		9.780	2.689	0.275

**Table 3.** Analysis of results of the four DEMs with the RSM.

Sensor Model	DEM	GCPs	DEM $\text{RMSE}_Z$ (m)	Orthoimage $\text{RMSE}_{XY}$ (m)	Ratio ( $\text{RMSE}_{XY}/\text{RMSE}_Z$ )
Refined RFM	KGPS-DEM	9	2.129	0.501	0.235
	Topo-DEM		3.581	0.997	0.279
	SRTM-GDEM		6.228	1.332	0.214
	ASTER-GDEM		9.780	2.593	0.265

**Table 4.** Analysis of results of the four DEMs with the refined RFM.

ranges from 0.563 to 2.689 m. On the other hand, Table 4 shows that there is a strong correlation between DEM vertical accuracy and the planimetric accuracy of the produced orthoimage. The higher the DEM  $RMSE_Z$  (low vertical accuracy), the higher the  $RMSE_{XY}$  of the generated orthoimage (low planimetric accuracy). In essence, this relation can be expressed as a ratio ( $RMSE_{XY}/RMSE_Z$ ). Under such an observation, the planimetric accuracy of the generated orthoimage is around the *quarter* of the vertical accuracy of the used DEM. This ratio approximately equals to the tangent of the off-nadir angle of the QuickBird image which equals  $15.5^\circ$  and this is consistent with the study by Jacobsen (2003), which showed that a discrepancy  $\Delta h$  in the height information of a DEM is

influencing the position  $\Delta L$  in an orthoimage by a ratio of

$$\Delta L = \Delta h \times \tan(\text{local nadir angle}).$$

As compared with the RSM, the refined RFM (Table 4) increases the accuracy only slightly with  $RMSE_{XY}$  ranges from 0.501 to 2.593 m. However, the strong correlation between DEM vertical accuracy and the planimetric accuracy of the produced orthoimage still can be observed. As well, the previously observed ratio between  $RMSE_{XY}$  and  $RMSE_Z$  still exists.

Figure 4 shows that the orthorectification process is greatly affected by the vertical accuracy of the applied DEM and they are directly correlated. In general, the two sensor models gave very close results. From the practical point of view, the

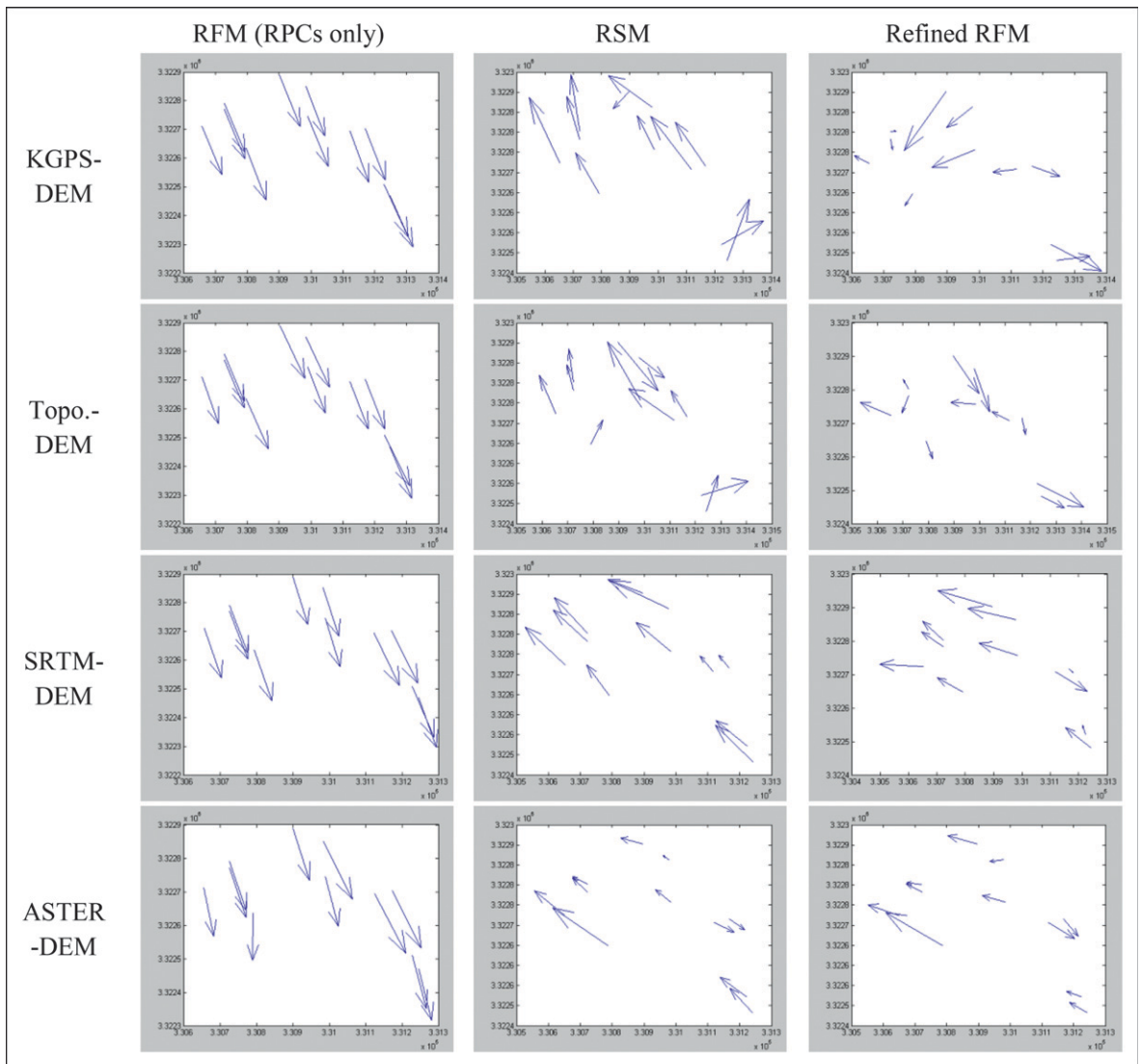


**Figure 5.** Vector plot of errors for the performance of different models with different DEMs.

results of the refined RFM are more stable and more precise than that of the RSM.

It is worth mentioning that in case of RFM (RPCs only), the orthoimages derived from SRTM and ASTER-DEMs are found to have planimetric accuracies on the order of 12.91-13.03 m, respectively. This level of accuracy is comparable to the level of accuracy obtained by KGPS-DEM and Topo-DEM, 13.68 and 13.83 m respectively. These results indicate that the RFM (RPCs only) is not sensitive to the vertical accuracy of the used DEMs.

On the other hand, in case of RSM and refined RFM, the accuracies derived from SRTM and ASTER-DEMs are significantly lower than the accuracies obtained by KGPS-DEM and Topo-DEM. However, these lower accuracies still can be used to produce base maps with excellent planimetric accuracies when flat areas are to be mapped.

In addition, the presence and value of systematic errors were evaluated. Figure 5 shows the spatial distribution of the used ChkPs for the comparison. In case of RFM (RPCs only), the spatial distribution of the differences clearly indicates a systematic error in the orthophoto production process. In case of RSM, the spatial distribution of the differences indicates systematic errors at the majority of points, whereas few points indicate no errors. In case of refined RFM, the spatial distribution of the differences indicates that the differences are not systematic, and hence no systematic biases have been occurred during the generation of the orthophotos.

## Conclusions and Recommendations

The research goal was to find out the impact of DEM's vertical accuracy on the planimetric accuracy of the generated orthoimage. A QuickBird satellite image of a level LV2A (standard), four different DEMs with different vertical accuracies, nine GCPs, and three sensor models has been applied. The results showed that the planimetric accuracy of the produced orthoimage is greatly affected by the vertical accuracy of the used DEM. In other words, the higher the DEM vertical accuracy, the higher the produced orthoimage planimetric accuracy. On the other hand, the planimetric accuracy of the produced orthoimages is around 0.25 of the vertical accuracy of the used DEM.

The RFM without using GCPs gives inaccurate results as the research showed that the RMSE<sub>XY</sub> of the four orthoimages produced using the RFM were 13.68, 13.83, 12.91, and 13.03 m using KGPS-DEM, Topo-DEM, SRTM-DEM, and ASTER-DEM, respectively. This remarkable low accuracy because of the disuse of GCPs as the RFM depends only on the approximate RPCs provided with the satellite image. The refined RFM is recommended when accurate results are expected, as the results showed that the planimetric accuracies of the four orthoimages produced using this model were 0.50, 1.00, 1.33, and 2.59 m using KGPS-DEM, Topo-DEM, SRTM-DEM, and ASTER-DEM, respectively.

Based on the results obtained in this research, several recommendations could be suggested for future work. It is recommended to carefully consider DEM's vertical accuracy for orthorectifying satellite images especially when high-resolution satellite images are used. As well, it is recommended to use either rigorous model or refined RFM with suitable number of GCPs to get reliable orthorectification results. Finally, it is recommended to evaluate further sources of DEMs such as synthetic aperture radar (SAR) and Light Detection and Ranging (LiDAR) data.

## REFERENCES

- Aguilar, M.A., F.J. Aguilar, J.A. Sánchez, F. Carvajal, and F. Agüera. 2005. Geometric correction of the Quickbird high resolution panchromatic images. In: *Proceedings of XXII International Cartographic Conference (ICC2005)*, A Coruña, Spain, July 11-16, 2005.
- Aguilar, M.A., F.J. Aguilar, F. Agüera, and J.A. Sánchez. 2007. Geometric accuracy assessment of QuickBird basic imagery using different operational approaches. *Photogrammetric Engineering and Remote Sensing* 73(12): 1321-32.
- Chang, W.C., L.C. Chen, and T.A. Teo. 2010. Collocation-aided adjustment of heterogeneous models for satellite images. In: W. Wagner and B. Székely (eds), *ISPRS TC VII Symposium—100 Years ISPRS*, July 5-7, 2010. Vienna, Austria: IAPRS, Vol. XXXVIII, Part 7B. ([http://www.isprs.org/proceedings/XXXVIII/part7/b/pdf/117\\_XXXVIII-part7B.pdf](http://www.isprs.org/proceedings/XXXVIII/part7/b/pdf/117_XXXVIII-part7B.pdf); accessed March 14, 2017).
- Di, K., R. Ma, and R.X. Li. 2003. Rational functions and potential for rigorous sensor model recovery. *Photogrammetric Engineering and Remote Sensing* 69(1): 33-41.
- Elashmawy, N., Y. Elmanadili, and B. Barakat. 2005. Comparative analysis and evaluation of various mathematical models for stereo IKONOS satellite

- images. FIG Working Week 2005 and GSDI-8 Cairo, Egypt, April 16-21, 2005.
- Giannone, F. 2006. *A rigorous model for high resolution satellite imagery orientation*. Rome, Italy: Faculty of Engineering, University of Rome La Sapienza.
- Hosseini, M. 2008. Analysis of rational function dependency to the height distribution of ground control points in geometric correction of aerial and satellite images. *The international archives of the photogrammetry, remote sensing and spatial information sciences*. Beijing, China: XXXX. Vol. XXXVII. Part B1. ([http://www.isprs.org/proceedings/XXXVII/congress/1\\_pdf/196.pdf](http://www.isprs.org/proceedings/XXXVII/congress/1_pdf/196.pdf); accessed March 14, 2017).
- Jacobsen, K. 2003. *Geometric potential of IKONOS and QuickBird images*. Heidelberg, Germany: The Photogrammetric Week.
- Junfeng, X., and H. Jingfeng. 2006. Orthorectification of IKONOS and impact of different resolution DEM. *Geo-spatial Information Science*, June 2006, Volume 9, Issue 2, pp. 108-111, Article ID: 1009-5020(2006)02-108-04.
- Li, D., J. Gong, Y. Guan, and C. Zhang. 2002. Accuracy analysis of digital orthophotos. In: *International Archives of Photogrammetry, Remote Sensing and Spatial Information Science*, Vol. XXXIV, Part 2, Commission II, August 20-23, 2002, Xi'an, China.
- Li, D., J. Shan, and J. Gong. 2009. *Geospatial technology for earth observation*. Wein, New York: Springer. (<https://link.springer.com/book/10.1007/978-1-4419-0050-0?no-access=true>; accessed March 14, 2017).
- Tao, C., Y. Hu, J. Mercer, S. Schnick, and Y. Zhang. 2000. Image rectification using a generic sensor model-rational function model. *The International Archives of Photogrammetry and Remote Sensing*, Vol. 33, Part B3, July 16-23, 2000, Amsterdam, The Netherlands. pp. 874-81.
- Tao, C.V., and Y. Hu. 2001. A comprehensive study of the rational function model for photogrammetric processing. *Photogrammetric Engineering and Remote Sensing* 67(12): 1347-57.
- Volpe, F., and L. Rossi. 2003. QuickBird high resolution satellite data for urban applications. *2nd GRSS/ISPRS Joint Workshop on Remote Sensing and Data Fusion over Urban Areas*, May 22-23, 2003, Berlin, Germany.
- Wu, W., L. Chen, and T. Teo. 2008. *RFM-based block adjustment for satellite images with weakly convergent geometry*. Chung-Li, China Taipei: Center for Space and Remote Sensing Research, National Central University. ([https://www.researchgate.net/publication/228726068\\_RFM-Based\\_Block\\_Adjustment\\_for\\_Satellite\\_Images\\_with\\_Weakly\\_Convergent\\_Geometry](https://www.researchgate.net/publication/228726068_RFM-Based_Block_Adjustment_for_Satellite_Images_with_Weakly_Convergent_Geometry); accessed March 14, 2017).